

Travel times in complex environments

Adrien DAGALLIER^(1,2), Sylvain CHEINET⁽¹⁾, Daniel JUVE⁽²⁾, Aurélien PONTE⁽³⁾, Jonathan GULA⁽³⁾

⁽¹⁾Institut de recherche franco-allemand de Saint-Louis, Saint-Louis 68300, France, adrien.dagallier@isl.eu

⁽²⁾Université de Lyon, Ecole Centrale de Lyon, Laboratoire de Mécanique des Fluides et d'Acoustique, Unité Mixte de Recherche, Centre National de la Recherche Scientifique 5509, Ecully F-69134, France

⁽³⁾Université de Brest, CNRS, IRD, Ifremer, Laboratoire d'Océanographie Physique et Spatiale (LOPS), IUEM, Brest 29280, France

Abstract

Times of Arrival (TOAs) of propagated signals are of utmost interest in seismic, underwater as well as aerial acoustics. From TOAs, one may reconstruct the propagation media properties from known sources and sensors positions, or conversely, find sound events locations in a known environment. Modeling the TOAs in realistic environments (wind or current, sound speed gradients, obstacles...) requires a general physical model, able to factor in the impact of refractive and diffractive processes. We present an interface-tracking model based on Sethian's Fast-Marching method for computing TOAs. This method is applicable to complex, 3D meshed environments. Examples will be given in the open atmosphere, in the ocean, as well as in an urban environment. Keywords: Fast-Marching, propagation, simulation, time of arrival, time matching

1 INTRODUCTION

Propagation through complex media alters the acoustic signature of a signal. The amplitude of the signal may be increased or strongly dampened, the frequency content may change. Working with and interpreting complete time series therefore represents a challenge. However altered the measured acoustic signature of an impulse sound might be, Times of Arrival (TOAs) may most of the time still be extracted. Despite their apparent simplicity, TOAs carry a lot of useful information about the propagation medium. They are widely used for source localization [1, 2] or acoustic tomography applications through comparison between measurements and model predictions. The more physically accurate the propagation models, the more information about the medium may be taken advantage of.

Many modelling approaches have been investigated throughout the years in the different acoustic communities. The evolution of the available computational resources has paved the way for high resolution, 3D acoustic models in the time or frequency domains. The cost of these simulations remains however prohibitive as soon as numerous simulations are required.

Lighter and faster methods have thus been developed. Ray tracing methods (high frequency approximation) with various degrees of physical realism and mathematical complexity have been proposed, but multipaths and shadow zones remain a critical issue. Gaussian beams approaches have overcome some of these limitations while bringing up new questions.

Starting from the end of the 80's, methods predicting TOAs in a whole domain have emerged in the seismic community. These methods are based on Huyghens principle and draw upon graph theory algorithms (Dijkstra algorithm) to compute the TOAs in a grid very effectively in a single-pass fashion. The TOAs thus predicted are the first TOAs, and the first TOAs only. TOAs coming from e.g. reflections are not computed. A further improvement is brought about in the 90's with the mathematical viscosity solution theory, which provides a suitable theoretical framework for obtaining the first TOAs in arbitrarily complex environments, at a small computational cost. The resulting methods have been called Fast-Marching or Ordered Upwind methods.

This paper presents a framework to predict first times of arrival throughout meshed domain: Cartesian grids, curvilinear meshes and general unstructured meshes. We name it the IFM, for Institute Saint-Louis Fast-

Marching Model. In the next section, the IFM model is introduced briefly. Examples of propagation through a complex atmosphere, the ocean and an urban environment are presented in section 3. Section 4 concludes.

2 ACOUSTIC MODEL

Instead of computing the full 3D pressure field at every point of the meshed domain, the IFM tracks a simple wavefront. Let c and \mathbf{w} be the medium sound speed and 3D wind (or current), respectively. Let \mathcal{T} be the first TOA throughout the domain. The TOAs in the domain may be obtained by solving Eq. (1):

$$\|\nabla\mathcal{T}\| \times \left(c + \mathbf{w} \cdot \frac{\nabla\mathcal{T}}{\|\nabla\mathcal{T}\|} \right) = 1. \quad (1)$$

The isosurfaces of \mathcal{T} may be seen as the acoustic wavefronts at given propagation times.

In this study, we use a solver of Eq. (1) based on the model of Sethian and Vladimirovsky [3], extended to 3D and Cartesian and curvilinear meshes. This choice is motivated by the generality of their formulation. It addresses general anisotropic problems, where the wavefront propagation depends not only on the position of the front, but also on the direction of propagation [3, 4], e.g. wind, for application in atmospheric acoustics, or currents in underwater acoustics. This approach readily applies to seismic acoustics [5, 6] or underwater acoustics [7].

The IFM propagates these wavefronts from an initial “known” subdomain, e.g. a single point for an acoustic point source. Let us define the interface between the “known” and the “unknown” subdomains as the set of points at the boundary of the “known” domain. The IFM then finds the point with the smallest TOA in the interface which is transferred to the “known” domain, compute its neighbors’ TOAs and add them to the interface. The TOAs are computed from the “known” points, by means of Eq. (1). The algorithm stops when all points are “known”.

Numerically speaking, the equation has to be approximated on a discrete arbitrary mesh. Let \mathbf{v} be the discrete approximation of $\nabla\mathcal{T}$. One has: $\mathbf{v} \simeq P\nabla\mathcal{T}$. The matrix P is calculated from the “known” neighbors positions (it is therefore position-dependent) and will be explicitated in the different cases of Sec. 3.

Equation (1) may therefore be rewritten, following Sethian and Vladimirovsky [3], as (with the notation $A^T = \text{transpose of } A$):

$$\mathbf{v}^T (PP^T)^{-1} \mathbf{v} \times \left(c + \mathbf{w} \cdot \frac{P^{-1}\mathbf{v}}{\|P^{-1}\mathbf{v}\|} \right)^2 = 1. \quad (2)$$

In theory, refining the mesh makes the solution converge to the viscosity solution. It is however not always practical for large computation domains, and may be balanced by use of higher order upwind stencils for \mathbf{v} .

The gradient \mathbf{v} coefficients depend on the TOA value of the neighbors and of the coefficients of the chosen finite difference scheme [3, 5, 8].

In isotropic cases (no wind, $\mathbf{w} = \mathbf{0}$), this equation reduces to a standard quadratic equation and may be solved analytically. In anisotropic cases ($\mathbf{w} \neq \mathbf{0}$), an iterative solver is required. Anisotropy is accounted for by a retroaction loop [9] and the implementation of Yatziv *et al.* [10] is retained for its linear scaling of the computation time and the number of points.

The IFM has been validated against Finite-Difference Time Domain simulations (FDTD) of an impulse signal in a domain with obstacles and strong sound speed contrasts. The IFM wavefront and the FDTD simulations coincide everywhere, including behind obstacles where only diffracted waves propagate [2].

3 APPLICATIONS

The acoustic model may further be adapted to different kind of meshes depending of the scenario. This section presents applications to propagation

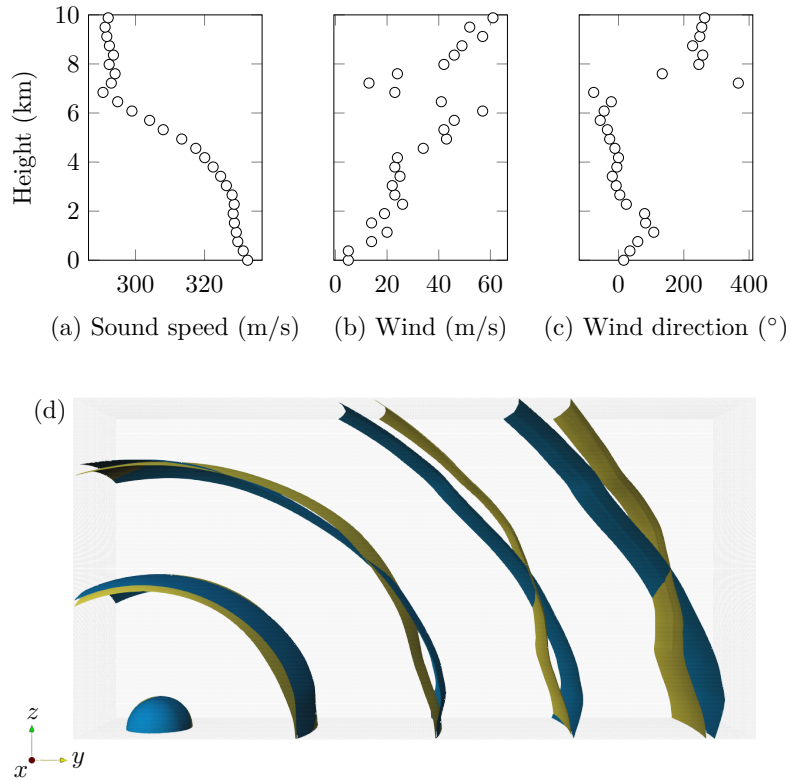


Figure 1. (a-c) Examples of measured atmospheric profiles somewhere in North Germany, in February. (d) Propagation of acoustic wavefronts in the atmosphere defined by the (a-c) data (blue wavefront) and the (a-c) data with reversed wind (yellow wavefront). The simulation domain is $20 \text{ km} \times 10 \text{ km} \times 4 \text{ km}$ in the y , z and x direction, respectively.

- in a complex atmosphere,
- in the ocean,
- in an urban environment.

3.1 Atmosphere

The model of the previous section is run here on a 40 million points $20 \text{ km} \times 10 \text{ km} \times 4 \text{ km}$ Cartesian domain. The computation takes a few minutes on a single CPU. Second order upwind finite difference are used [5]. The neighbors of any given points are one grid step away in each dimension, the matrix P is diagonal.

The atmosphere through which the wavefronts propagate is shown on Figure 1. The curvature of the wavefronts may be linked to the changes in the wind and temperature profiles. It is thus possible to account for the anisotropic effect of the wind on sound propagation. As mentioned in the previous section, an analytical solution is possible in the absence of wind, which drastically improves the speed of the calculation (from about 130,000 points/s to more than 1 million points/s).

The wavefronts propagate in an atmosphere with an upward refracting atmosphere due to the sound speed profile and the wind profiles up to 6 km. This creates a so-called shadow zone. As opposed to ray tracing techniques,

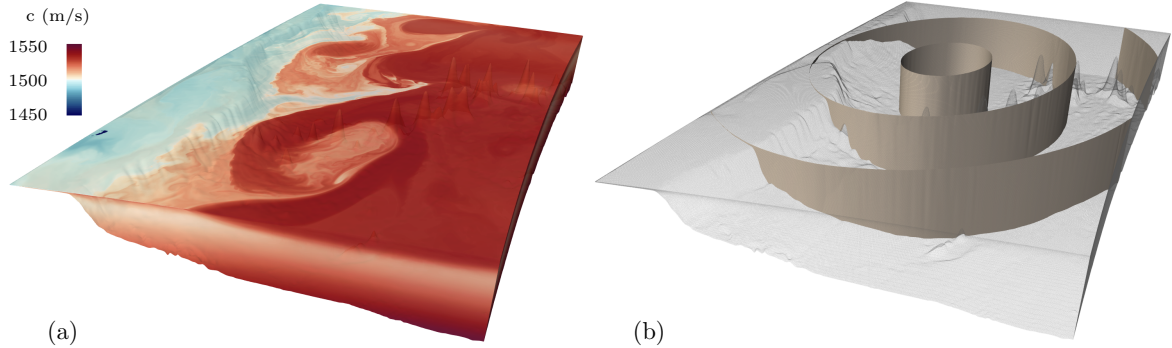


Figure 2. (a) Sound speed c in the ocean, close to the US Eastern coast. The vertical dimension has been stretched by a factor 50. (b) Snapshots of the acoustic wavefront from an impulse source close to $(40N, -68W)$ after 70, 200 and 330 seconds of propagation.

the IFM is able to predict TOAs in these regions. However, only the wavefront is computed. Information regarding the amplitude is not accounted for by the model. It is therefore possible that the model would predict TOAs that might not actually be measured, depending on the frequency content of a given signal, or on how deep into the shadow zone the receiver is. A prior physical analysis is required to define the region in which the model results are meaningful for comparison to experimental data.

3.2 Ocean

The method is now applied to first TOA determination in the ocean. The sound speed data from Figure 2a are the output of a realistic ROMS simulation for a $1000 \text{ km} \times 800 \text{ km}$ region, close to the US East coast. The simulation domain has 2000×1600 points and 50 terrain-following vertical levels. It is forced by realistic surface forcings and boundary ocean data from a coarser resolution model. More details may be found in Gula *et al.* [11]. The high sound speed at the surface is due to the warm Gulf Stream current off New England. The data are given on a 160 million points terrain-following curvilinear mesh, and also include the 3D velocity field (not shown).

The IFM is extended to curvilinear meshes for propagation on terrain-following meshes. The formalism is exactly the same as in the previous sections. Only the matrix P changes, and must now be expressed in term of the Jacobian matrix of the curvilinear transform [12]. The computation time on a single CPU, is of around 90 minutes (30,000 points/s), due to the heavier computations involved (Jacobian matrices to inverse) and to our specific implementation, which prioritizes low memory usage over efficiency. The code runs on a 16GB laptop. An example of point source propagation is illustrated on Figure 2b. The “creasing” on the wavefronts is caused by the heterogeneity of the sound speed distribution. Even if the oceanic velocities are much smaller than the sound speed ($< 1 \text{ m/s}$ nearly everywhere vs. 1500 m/s), the propagation anisotropy may be observed as in the atmospheric case. It may therefore be possible to use the IFM for acoustic tomography of the ocean.

3.3 Urban environments

The method is now applied to an urban propagation scenario. The considered domain is of size $170 \text{ m} \times 170 \text{ m} \times 20 \text{ m}$ (Figure 3). To take into account the variety and the complexity of the shape of the building, extension of the IFM to unstructured meshes is carried out, extending ref. [3] to 3D. The matrix P rows now contain the vectors connecting the current point to its neighbors.

As the algorithm requires only the list of the neighbors for each mesh point, the mesh may feature any kind of 3D element (tetrahedron, pyramid, hexahedron...). High order gradient computations are however much more

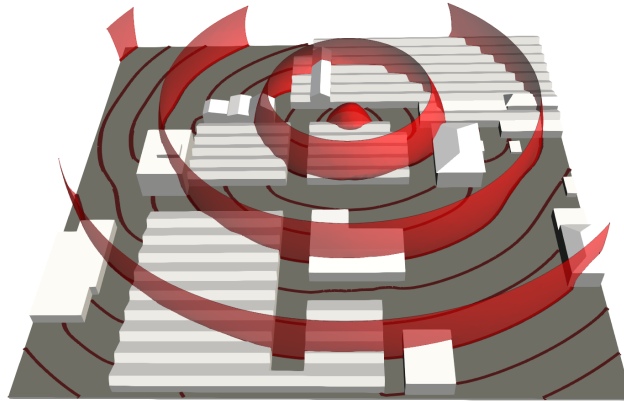


Figure 3. Snapshots of acoustic propagation of a point source in a realistic urban environment. Domain size is 170 m×170 m×20 m. The brown lines are the ground-level values of the TOAs wavefronts.

difficult to implement. They are furthermore not always necessary, since the mesh may be refined, e.g. close to the sound source and along building edges to enhance the computation accuracy.

The lines on the ground illustrate the effects of the environment on the TOAs. Corrections of the order of up to several hundred ms may be expected compared to direct propagation in straight line, which may be seen as sensor positioning uncertainties of several meters.

4 CONCLUSIONS

The IFM interface-tracking framework presented in this article is a very general framework for predicting TOAs in arbitrarily complex environments. It may be applied on various types of mesh, from regular Cartesian to curvilinear grids, to unstructured meshes. High order schemes for TOA computation may be used when precision is of the essence. Application to ocean or atmospheric acoustics are considered. The IFM may therefore be used for a general set of applications that require first TOAs in realistic 3D media with non-flat ground or bottom and arbitrary medium properties, such as source localization or acoustic tomography.

The IFM is further not limited to point sources. Elongated sources (such as the Mach waves generated by supersonic projectiles or aircrafts) may also be treated in an identical way [2].

It should however be kept in mind that the signal amplitude is not accounted for by the model. At large distances or deep in shadow zones, the framework may numerically predict TOAs that cannot be measured experimentally, because of too low a signal amplitude or too high a noise level. The physical validity limits have to be defined for each specific application.

REFERENCES

- [1] Cheinet, S.; Ehrhardt, L.; Broglin, T., Impulse source localization in an urban environment: Time reversal versus time matching, *The Journal of the Acoustical Society of America*, **139**(1), 2016, pp 128-140
- [2] Dagallier, A.; Cheinet, S.; Wey, P.; Rickert, W.; Weßling, T.; Juvé, D., Acoustic localization of artillery shots, 6th Workshop on Battlefield Acoustics, Saint-Louis, France, 2018
- [3] Sethian, J. A.; Vladimirsky, A. B., Ordered Upwind Methods for static Hamilton-Jacobi equations: theory and algorithms, *SIAM Journal on Numerical Analysis*, Vol 41 (1), 2003, pp 325-363.

- [4] Sethian, J. A, A fast marching level set method for monotonically advancing fronts, Proceedings of the National Academy of Sciences, **93**(4), 1996, pp 1591-1595
- [5] Popovici A.; Sethian, J. A, 3D imaging using higher order Fast Marching travel times, Geophysics, **67**(2), 2002, pp 604-609
- [6] Sethian, J. A; Popovici A., 3D travel time computation using the Fast Marching method, Geophysics, **64**(2), 1999, pp 516-523
- [7] Pailhas, Y.; Petillot, Y., Multi-dimensional Fast-Marching approach to wave propagation in heterogeneous multipath environment, Third Underwater Acoustics Conference and Exhibition, Platanias, Crete, Greece, 2015
- [8] Sethian, J. A; Vladimirov, A. B., Fast methods for the Eikonal and related Hamilton-Jacobi equations on unstructured meshes, Proceedings of the National Academy of Sciences, **97**(11), 2000, pp 5699-5703
- [9] Konukoglu, E.; Sermesant, M.; Clatz, O.; Peyrat, J.-M.; Delingette, H.; Ayache, N., A recursive anisotropic Fast Marching approach to reaction diffusion equation: application to tumor growth modeling, In: Karssemeijer, N., Lelieveldt B. (eds) Information Processing in Medical Imaging, 2007, Lecture Notes in Computer Science, vol. 4584, Springer Berlin Heidelberg
- [10] Yatziv, L.; Bartesaghi, A.; Sapiro, G., O(N) implementation of the fast marching algorithm, Journal of Computational Physics, **212**(2), 2006, pp 393-399
- [11] Gula, J.; Molemaker, M. J.; McWilliams, J. C., Gulf stream dynamics along the Southeastern U.S. Seaboard, Journal of Physical Oceanography, **45**(3), 2015, 690-715
- [12] Visbal, M.; Gaitonde, D., On the Use of Higher-Order Finite-Difference Schemes on Curvilinear and Deforming Meshes, Journal of Computational Physics, **181**(1), 2002, pp 155-185